

Nonlinearity sensing via photon-statistics excitation spectroscopy

Marc Aßmann and Manfred Bayer

Experimentelle Physik 2, Technische Universität Dortmund, D-44221 Dortmund, Germany

(Received 29 August 2011; published 3 November 2011)

We propose photon-statistics excitation spectroscopy as an adequate tool to describe the optical response of a nonlinear system. To this end we suggest to use optical excitation with varying photon statistics as another spectroscopic degree of freedom to gather information about the system in question. The responses of several simple model systems to excitation beams with different photon statistics are discussed. Possible spectroscopic applications in terms of identifying lasing operation are pointed out.

DOI: [10.1103/PhysRevA.84.053806](https://doi.org/10.1103/PhysRevA.84.053806)

PACS number(s): 42.50.Ar, 42.62.Fi, 78.47.D–

I. INTRODUCTION

According to Glauber, an adequate description of the degree of coherence of a light field is given by the second-order correlation function [1]

$$g^{(2)}(\tau) = \frac{\langle \hat{a}^\dagger(t) \hat{a}^\dagger(t+\tau) \hat{a}(t) \hat{a}(t+\tau) \rangle}{\langle \hat{n}(t) \rangle \langle \hat{n}(t+\tau) \rangle}, \quad (1)$$

where \hat{a}^\dagger and \hat{a} denote photon creation and annihilation operators of the mode of interest, t gives the detection time of the first photon, and τ is the time delay until the detection of the second photon. Basically, this quantity describes the probability of detecting two photons of a light field at times t and $t+\tau$ compared to the probability of detecting two photons for a light field of the same mean intensity, but statistically independent photon detection events. It is therefore a measurement of the relative variance of a photon number distribution. As a consequence, the most accurate description of a light field is given by a hierarchy of such functions up to arbitrary order which correspond to measurements of the higher-order moments of a photon number distribution. While photon number statistics are used quite regularly to characterize the emission from a system, most prominently for identifying single-photon sources [2], the buildup of coherence in lasers [3,4] or Bose-Einstein condensates [5,6], and in dynamic light scattering [7] or fluorescence correlation spectroscopy [8], they are currently not routinely used as a spectroscopic tool, although the important effect of the excitation photon statistics on the excited quasiparticles has been highlighted [9,10] and there have been theoretical predictions for excitation photon-statistics dependencies of several quantities, for example, excitation efficiencies of optically active excitons in nanostructures [11]. The most probable reason for neglecting this degree of freedom in experiments lies in the small amount of light sources which offer tunable photon statistics, although recently advances in this direction have been made experimentally [6,12,13] and theoretically [14–16].

It is widely known and well studied that almost every kind of optical amplification adds noise to the amplified signal [17]. In this paper we are interested in approaching this phenomenon from the other side and aim at identifying nonlinearities in the optical response of the system in terms of the output signal photon statistics in dependence on the input signal photon statistics. To clearly demonstrate the influence of nonlinearities on the output photon statistics, we choose to study a simple nonlinear system which nevertheless demonstrates all essential

features: a phase-insensitive system giving a sigmoidal response superimposed on a linear response. The average output photon number of such a system is given by

$$\langle n_{\text{out}}(n_{\text{in}}) \rangle = Ln_{\text{in}} + \frac{S}{1 + e^{-(n_{\text{in}} - N)}}, \quad (2)$$

where L gives the slope of the linear response, S gives the magnitude of the nonlinear sigmoidal step, and N denotes the threshold input photon number of the nonlinearity. In experiments on nonlinear optical systems, this response function is usually not directly probed, but rather the response to a mean input $\langle n_{\text{out}}(\langle n_{\text{in}}) \rangle$ is investigated in terms of input-output curves. Higher-order responses beyond the mean output photon numbers are also examined in experiments in terms of second- and higher-order photon number correlation functions of the output signal [18,19]. These allow one to distinguish between systems which give the same $\langle n_{\text{out}} \rangle$ at a given $\langle n_{\text{in}} \rangle$, but show different underlying photon number statistics, resulting in larger or smaller photon number fluctuations.

II. PHOTON NUMBER STATISTICS

The three most widely known kinds of photon number distributions commonly found in real systems are coherent states in lasers, thermal states in thermal emitters, and Fock states as seen for photon number state sources, which are for stationary fields characterized by values of $g^{(2)}(0)$ equal to unity, 2, or $1 - \frac{1}{\langle n \rangle}$, respectively. The probability to detect exactly n photons for a mean photon number $\langle n \rangle$ is given by a Poisson distribution

$$p_{(n),\text{coh}}(n) = e^{-\langle n \rangle} \frac{\langle n \rangle^n}{n!} \quad (3)$$

in the coherent case, a Bose-Einstein distribution

$$p_{(n),\text{th}}(n) = \frac{1}{(1 + \langle n \rangle)(1 + \frac{1}{\langle n \rangle})^n} \quad (4)$$

in the thermal case, and a sub-Poissonian distribution

$$p_{(n),\text{Fock}}(n) = \begin{cases} 1 & \text{if } n = \langle n \rangle, \\ 0 & \text{else} \end{cases} \quad (5)$$

for Fock number states. Nevertheless, the optical response of these systems to an optical excitation will not only depend on the mean photon number of the excitation light field, but also on its statistical properties. The response of a system as described by Eq. (2) for a given mean input photon number may therefore

differ depending on the underlying input photon number distribution. This opens up the possibility to characterize such systems in detail spectroscopically by varying the input photon number statistics. To this end, we theoretically investigate three systems which share the same mean output photon numbers according to Eq. (2), but give either a Poissonian distribution around this mean, a Bose-Einstein distribution around this mean, or a Fock state as a response, and study how the output photon numbers and correlation functions vary for inputs which also show a fixed mean photon number, but show variances according to Poissonian, Bose-Einstein, and Fock distributions for different values of S and N . The same linear slope $L = 1$ has been used for all calculations. We start with the linear case $S = 0$. The input-output curves are obviously the same for all nine possible combinations of input photon statistics and system responses. One of these linear curves is shown in Fig. 2 for comparison to other systems. The photon statistics for the different cases, however, differ. In the following, we use the terms $g_{in}^{(2)}$ for the photon statistics of the input light field, $g_{sys}^{(2)}$ for the statistics of the nonlinear system, and $g_{out}^{(2)}$ for the photon statistics of the output light field, and focus on equal time correlation functions only. The results are shown in Fig. 1. Here and in the following figures the nine possible combinations of Fock, coherent and thermal (labeled by the characters F, C, and T, respectively) excitation and system response are expressed as a set of two characters, where the first character denotes the excitation photon number statistics and the second represents the system response statistics. As expected, the output photon statistics of systems excited with Fock states are not distorted and stay Fock, Poissonian, or Bose-Einstein distributions, respectively. In analogy, also systems giving a Fock response preserve the input photon statistics. In all other cases some distortions occur as the total variance V_{out} of the output photon number distribution behaves roughly as

$$V_{out} \approx V_{sys} + g_{sys}^{(2)} V_{in}. \quad (6)$$

This distortion is only present for small input photon numbers if both of the statistics of the input light field and the nonlinear system are Poissonian. Already for intermediate photon numbers, the distribution recovers to the Poissonian limit of $g_{out}^{(2)} = 1$. The situation is similar if one of the two photon statistics is Poissonian and the other is thermal. In these cases the photon number noise increases at small mean input photon numbers according to Eq. (6) and recovers to the thermal limit of $g_{out}^{(2)} = 2$. In the case where both statistics are thermal, the situation changes. Although there is also a photon-number-dependent contribution which vanishes with increasing mean input photon number, the output photon number noise saturates at $g_{out}^{(2)} = 4$, which is much higher than the initial noise of the input photon field. This behavior is not surprising or unexpected. Basically all constant contributions beyond unity can be traced back to quadratic terms in the variances, while those terms depending on mean input photon numbers correspond to linear terms in the variances. However, the results already show that the output photon statistics are very sensitive to the response of the system if thermal excitation is used. It might seem surprising that the noise overshoot depending on $\langle n_{in} \rangle$ is usually not observed in

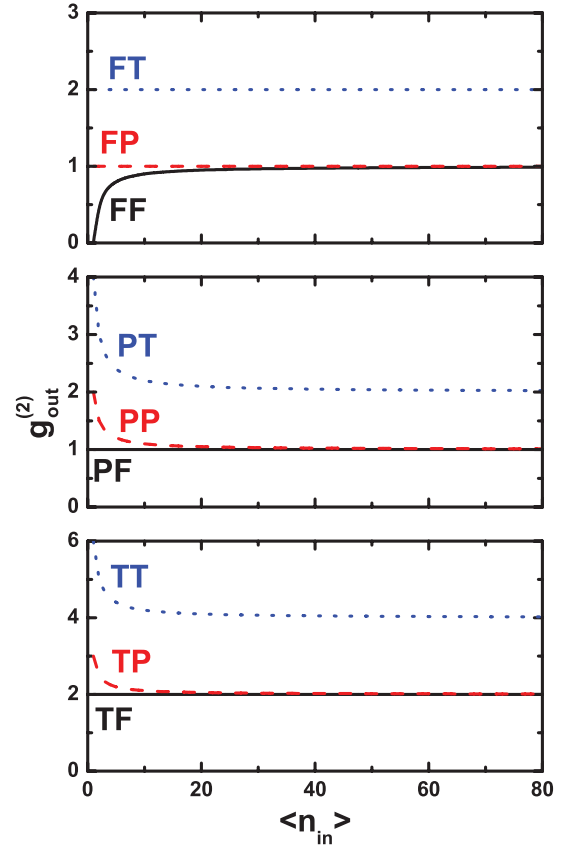


FIG. 1. (Color online) Output photon statistics for different linear systems and varying excitation conditions. The upper panel shows excitation with Fock states, the middle panel represents excitation using coherent states, and the lower panel corresponds to excitation with thermal states. The black solid lines represent systems giving a Fock distribution, the red dashed lines represent Poissonian distributions, and the blue dotted lines mark Bose-Einstein distributions.

experiments on coherent or thermal systems using laser pulses with Poissonian photon number distributions for excitation. Obviously our choice of $L = 1$ for the linear slope characterizes an ideal system. This value has been chosen for reasons of clear demonstration of the effects we predict. For any experiment on a real system such as a laser, this value will be much smaller and the output photon number using excitation pulses containing only few photons is too small to allow for sensible measurements of photon statistics under most circumstances.

III. NONLINEARITIES AND NOISE

Let us now focus on the effects of introducing a nonlinear response. We demonstrate the difference at a system with parameters of $L = 1$, $N = 45$, and $S = 50$. While the input-output (IO) curve is not sensitive to the statistics of the nonlinear system, the excitation photon number statistics will have an influence on the IO curve. This effect can be seen in Fig. 2. Here, the black solid line gives the IO curve using Fock excitation. The red dashed line gives the corresponding IO curve using coherent excitation. Obviously, the step in the IO curve becomes smeared out. This behavior is a consequence of

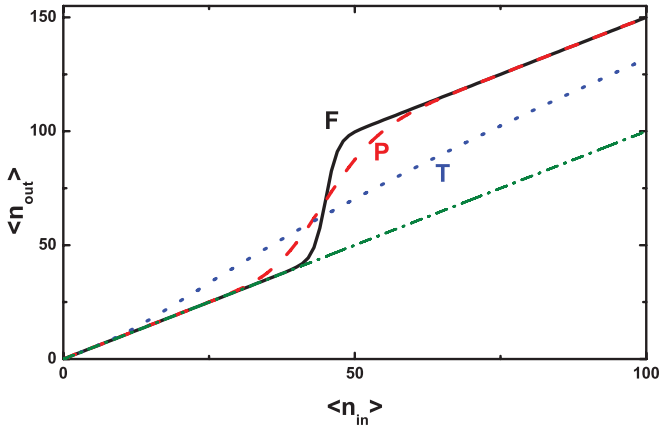


FIG. 2. (Color online) Input-output curves for parameters of $L = 1$, $N = 45$, and $S = 50$ at varying excitation photon statistics. The green dash-dotted line shows the curve for $S = 0$ for comparison. The undistorted IO curve using Fock-state excitation is shown in black. The excitation photon number distributions with larger variance tend to smear out the steplike jump in the IO curve, as can be seen for coherent (red dashed) and thermal (blue dotted) excitation.

the larger photon number variance of the coherent excitation. As the photon number will fluctuate around the mean value, the nonlinear response of the system already contributes at mean photon numbers below the nonlinear threshold. This effect is even stronger for excitation with thermal light. As the photon number variance is even larger in this case, the nonlinear region is broadened drastically and smeared out. Identifying the step in the IO curve may become rather difficult in this case. Also it should be noted that for large input photon numbers even far beyond the step in the IO curve, the mean output photon number for thermal excitation is much smaller than for Fock-state or coherent excitation. This behavior is also a consequence of the properties of the different excitation photon number distributions. The most probable photon number corresponds to the mean photon number for Fock-state or coherent excitation, and the fluctuations around this mean are zero or small, so that for mean input photon numbers beyond the threshold region also the actual input photon number for each repeated excitation will be larger than the threshold value. For thermal light, however, the most probable input photon number is always zero. In this case, even for $\langle n_{in} \rangle$ way beyond the threshold region, the actual input photon number for some of the repeated excitations will still be below the threshold. Consequently, $\langle n_{out} \rangle$ will be smaller compared to Fock-state or coherent excitation. The green dash-dotted curve gives the IO curve of a linear system for comparison. Although the suppressed step in the IO curve looks as an indicator that excitation using thermal light is not a suitable tool to characterize nonlinear systems, it is instructive to study the output photon number statistics, too. For the same choice of parameters the output photon statistics for all nine combinations of input photon statistics and system response statistics are shown in Fig. 3. As expected, no differences from the linear system are seen for excitation using Fock states. For excitation using Poissonian photon statistics, however, a small peak occurs in $g^{(2)}$ in the vicinity of the threshold. The relative

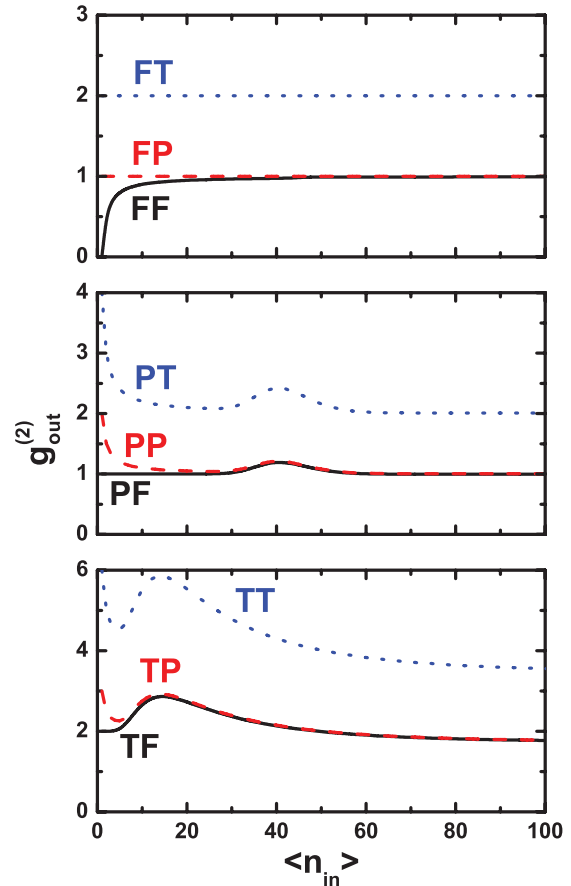


FIG. 3. (Color online) Output photon statistics for nonlinear systems with parameters of $L = 1$, $N = 45$, and $S = 50$ and varying excitation conditions. The upper panel shows excitation with Fock states, the panel in the middle shows excitation using coherent states, and the lower panel represents excitation with thermal states. The black solid lines represent systems giving a Fock distribution, the red dashed lines represent Poissonian distributions, and the blue dotted lines mark Bose-Einstein distributions.

magnitude of this peak is equal for all three possible system response statistics and amounts to an excess of $\sim 20\%$ beyond the value taken for a linear system. This highest value occurs at an input photon number $\langle n_{in} \rangle = 40$, which corresponds to the lower border of the threshold region. This increased noise peak can be seen in the region between $\langle n_{in} \rangle = 30$ and $\langle n_{in} \rangle = 60$, which equals the region in which the IO curve for coherent excitation differs from the bare response of the system, as seen for Fock-state excitation. Therefore, the increased output photon number noise can be explained by the variance of the input photon number. For each repeated excitation $\langle n_{in} \rangle$ will differ and the amplification by the nonlinearity will have a different magnitude. Accordingly, the added noise is largest when the mean photon number reaches the onset of the threshold as the amplification ratios vary strongly and decreases afterward because the spread in the nonlinearities experienced in each repeated excitation becomes smaller. A similar effect can be observed for excitation using thermal light. However, the effect differs significantly from the one predicted for coherent excitation. Here the relative magnitude of the excess noise peak is on the order of $\sim 45\%$ and is

thus larger. Also, the $\langle n_{in} \rangle$ at which the peak is reached is shifted to much smaller values. Here the peak is located at $\langle n_{in} \rangle = 14$, which is approximately one third of the threshold photon number. Basically this effect can be explained similarly to the case of coherent excitation. However, the much larger variance of $\langle n_{in} \rangle$ causes the output photon number noise to be much larger. The large input photon number variance also means that the nonlinear region is reached in a non-negligible percentage of repeated excitations already at $\langle n_{in} \rangle$ far below the threshold of the nonlinearity. Also it should be noted that thermal excitation shows an effect way beyond the threshold region. While for linear systems $g_{out}^{(2)}$ saturates at values of 2 or 4 depending on the response of the system, $g_{out}^{(2)}$ decreases further down to values of ~ 1.8 or 3.6 beyond the threshold region for the nonlinear system considered here. This drop in the output photon number noise is a consequence of the nonlinearity, effectively increasing the probability of intermediate and high output photon numbers slightly and therefore shifting the output photon number distribution toward an uniform distribution for which $g_{uni}^{(2)} = \frac{4}{3} - \frac{1}{\langle n_{out} \rangle}$ would be the expected outcome. It should further be noted that $g_{out}^{(2)}$ for the nonlinear system reaches the value of the linear system exactly at the upper end of the threshold region.

IV. EFFECT OF NONLINEARITY PARAMETERS

This peculiar behavior opens up the interesting possibility of identifying nonlinearities in a system at low excitation densities far before the nonlinear threshold is reached on average using excitation with thermal light. At this point, it is worthwhile to study to what extent the position and magnitude of those excess fluctuations depend on the choice of parameters. To this end, we also studied a system with a lower threshold photon number. The parameters used are $L = 1$, $S = 50$, and $N = 20$. The results are shown in Fig. 4. Qualitatively, the curves are similar to the ones shown before, but quantitative differences are present. For coherent and thermal excitation, excess peaks in $g_{out}^{(2)}$ can be seen again. For coherent excitation the maximum of the peak is still located at the lower border of the threshold region, and the peak value is enhanced approximately by 50% compared to a linear system. For thermal excitation these effects are even more pronounced for this set of parameters. The relative magnitude of the noise enhancement is slightly larger than 100%. The peak is reached at $\langle n_{in} \rangle = 5$, which is one third of the onset of the nonlinearity and one quarter of its middle. For thermal excitation and large $\langle n_{in} \rangle$, $g_{out}^{(2)}$ decreases even further down to values of 1.6 and 3.2, respectively. The $\langle n_{in} \rangle$ at which the values of 4 and 2 expected for the linear system are reached for the nonlinear system again correspond to the upper limit of the threshold region. The results remain qualitatively similar for any choice of S , as shown in Fig. 5, which shows the peak excess bunching $g_{out}^{(2)}(S) - g_{out}^{(2)}(S = 0)$ as a function of the nonlinear step size. The black solid and red dashed lines correspond to coherent excitation and a Poissonian or thermal nonlinearity, respectively. The blue dotted and green dash-dotted lines correspond to thermal excitation and a Poissonian or thermal nonlinearity, respectively. As expected, this difference gets larger for any combination of excitation

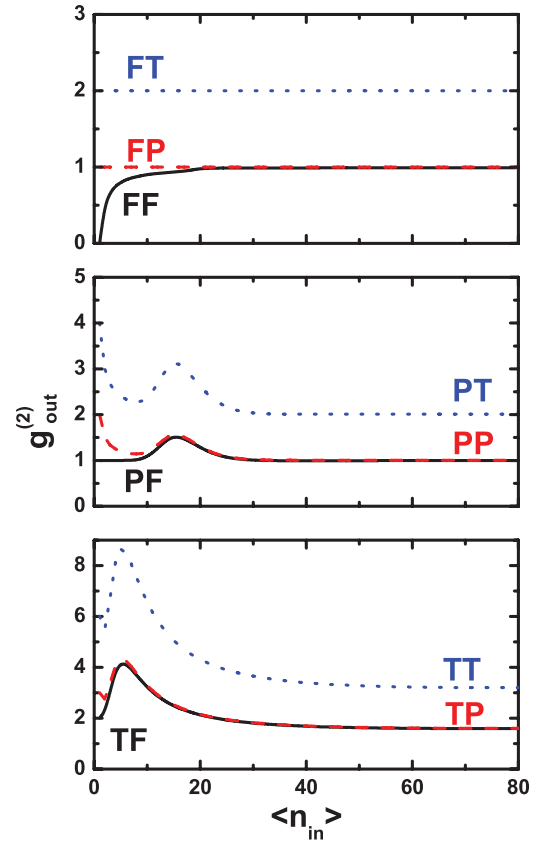


FIG. 4. (Color online) Output photon statistics for nonlinear systems with parameters of $L = 1$, $N = 20$, and $S = 50$ and varying excitation conditions. The upper panel shows excitation with Fock states, the middle panel represents excitation using coherent states, and the lower panel corresponds to excitation with thermal states. The black solid lines represent systems giving a Fock distribution, the red dashed lines represent Poissonian distributions, and the blue dotted lines mark Bose-Einstein distributions.

and system statistics, with increased S showing a slightly superlinear slope. Irrespective of the excitation statistics used, $g_{out}^{(2)}(S) - g_{out}^{(2)}(S = 0)$ is twice as large for a system giving a Bose-Einstein distribution than for one giving a Poissonian distribution, still allowing one to distinguish between thermal and coherent systems in experiments.

The amount of noise introduced by a nonlinearity will of course also depend on the input photon number at the threshold. Figure 6 shows $g_{out}^{(2)}(S) - g_{out}^{(2)}(S = 0)$ for varying N and fixed values of $S = 30$ and $L = 1$. It is not surprising that the effect is most pronounced for small N and disappears for large N as $\frac{S}{N}$ is a good measure of the relative strength of the nonlinearity. While the excess noise indeed vanishes for large N and coherent excitation, it disappears much slower for thermal excitation and still shows a magnitude of ~ 0.4 if $\frac{S}{N} = 0.25$, which should be measurable. The reason for this enduring effect at large N can be seen clearly in Fig. 7. Here the input photon number $\langle n_{in,max} \rangle$ at which the peaks shown in Fig. 6 occur are displayed as a function of N for coherent excitation (black solid line) and thermal excitation (red dashed). While for coherent excitation $\langle n_{in,max} \rangle$ is almost as large as N , it increases with a much smaller slope for thermal

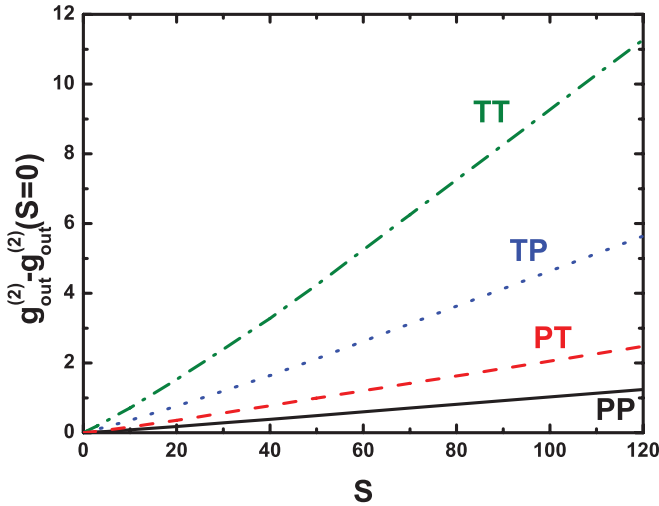


FIG. 5. (Color online) Maximum difference between $g_{\text{out}}^{(2)}$ for systems with varying S and $g_{\text{out}}^{(2)}$ for a system giving a linear response for $N = 20$. The black solid and red dashed lines correspond to coherent excitation and a Poissonian or thermal nonlinearity, respectively. The blue dotted and green dash-dotted lines correspond to thermal excitation and a Poissonian or thermal nonlinearity, respectively.

excitation. This outcome is in full agreement with the earlier result that, for thermal excitation, a peak in the output photon number occurs way below the threshold region. Now it is obvious that this overshoot in $g_{\text{out}}^{(2)}$ will be large when S is large compared to $\langle n_{\text{in,max}} \rangle$ and will vanish as $\langle n_{\text{in,max}} \rangle$ becomes larger than S , which requires very large values of N for thermal excitation.

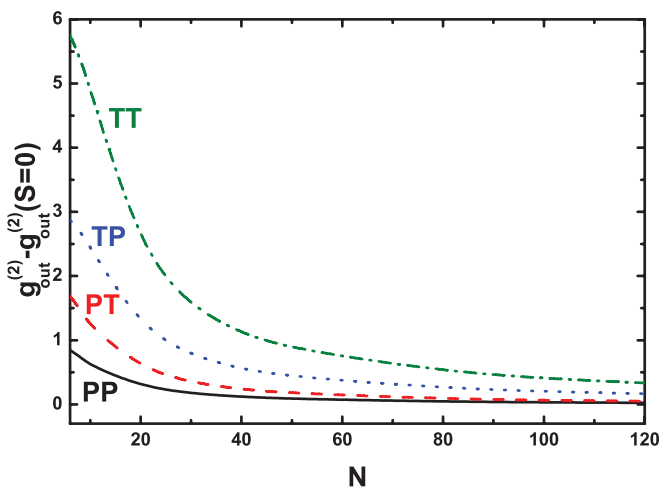


FIG. 6. (Color online) Maximum difference between $g_{\text{out}}^{(2)}$ for systems with varying N and $g_{\text{out}}^{(2)}$ for a system giving a linear response for $S = 30$. The black solid and red dashed lines correspond to coherent excitation and a Poissonian or thermal nonlinearity, respectively. The blue dotted and green dash-dotted lines correspond to thermal excitation and a Poissonian or thermal nonlinearity, respectively.

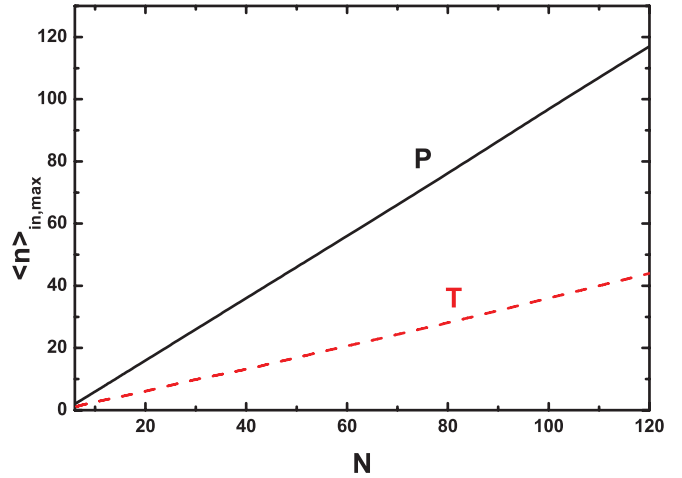


FIG. 7. (Color online) $\langle n_{\text{in,max}} \rangle$ at the maximum difference between $g_{\text{out}}^{(2)}$ for systems with varying N and $g_{\text{out}}^{(2)}$ for a system giving a linear response for $S = 30$. The black solid and red dashed lines correspond to coherent and thermal excitation, respectively.

V. EFFECTS ON LASERS

Let us now turn to the question under which circumstances the described effects might be observed in experiments. Considering, for example, lasers, the value N takes will depend strongly on the spontaneous emission factor β and the quality factor of that laser. For lasers with not too high β , S will scale as β^{-1} under steady-state conditions [20] because at the lasing threshold the fraction of all emission processes guided to the lasing mode increases from β to almost unity. A discussion of changes in the high- β regime, especially for semiconductor lasers, can be found in Ref. [21]. However, the onset of lasing occurs as the intracavity photon number reaches unity. Accordingly, N will also scale as β^{-1} for not too large β . Therefore, to get an impression for which kind of system one would expect significant changes in $g_{\text{out}}^{(2)}$, it seems reasonable to compare several systems where N and S are both scaled in fixed proportion to each other. Figure 8 shows the peak values of $g_{\text{out}}^{(2)}(S) - g_{\text{out}}^{(2)}(S=0)$ for several systems with $T = S = \beta^{-1}$ that can be considered to be role models for lasers showing different but still rather large β , but otherwise similar characteristics. The black solid and red dashed lines correspond to coherent excitation and a Poissonian or thermal non-linearity, respectively. The blue dotted and green dash dotted lines correspond to thermal excitation and a Poissonian or thermal nonlinearity. All four curves show only a weak dependence on β^{-1} . For coherent excitation a slight decrease of $\sim 35\%$ takes place over the two orders of magnitude examined here. However, the magnitude of the excess fluctuations is quite small. Taking into account the fact that for coherent excitation the peak value will occur in the nonlinear region, which is also the region where the system response statistics change from thermal to Poissonian for a common laser, it is very unlikely that these excess fluctuations can indeed be observed and clearly identified. For thermal excitation the excess fluctuations show an even weaker dependence on β^{-1} and a rather large magnitude. As these peak values occur far before the nonlinear region and therefore in a region where the system response statistics are assumed to be constant, it

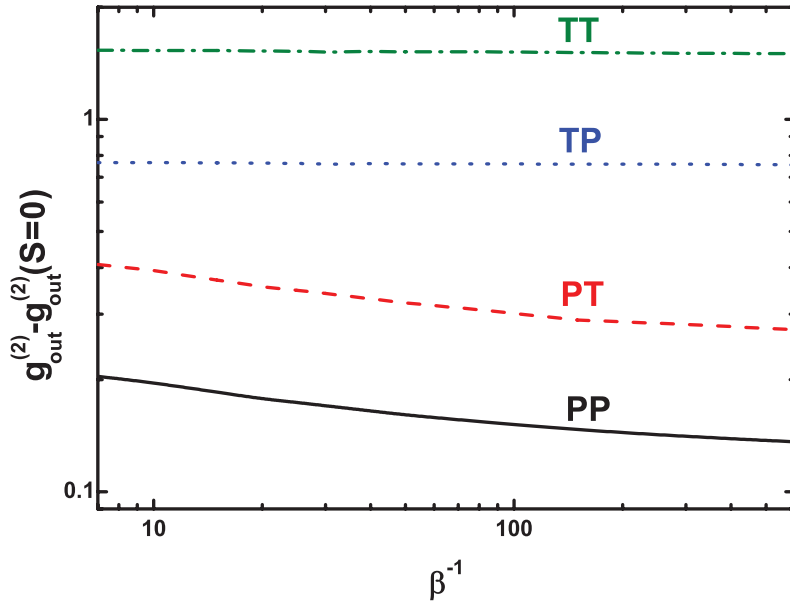


FIG. 8. (Color online) Maximum difference between $g_{\text{out}}^{(2)}$ for systems with varying β^{-1} and $g_{\text{out}}^{(2)}$ for a system giving a linear response shown on a double-logarithmic scale. The black solid and red dashed lines correspond to coherent excitation and a Poissonian or thermal nonlinearity, respectively. The blue dotted and green dash-dotted lines correspond to thermal excitation and a Poissonian or thermal nonlinearity, respectively.

should be possible to measure these excess fluctuations. This opens up the interesting possibility to identify and characterize a nonlinearity in a system response without the mean input photon number reaching the nonlinear threshold. Considering measurements on real systems, lasers with moderate or high values of β seem to be ideal candidates to examine these effects. For these lasers the threshold excitation density is not too high, which simplifies observation of the effects of thermal excitation as it is not a trivial task to create single-mode thermal light with high intensity. Application to real lasers should of course also take other factors into account which have been shown to have an influence on lasing operation. Examples are the probably more complicated shape of the input-output curves [21], the variation of the system response statistics from thermal to coherent along the lasing threshold [22], specific properties of the pumping process [23], nonstationary conditions [24], and specifics of the type of laser considered [25–27], which are out of the scope of this paper. We would like to point out that the lasing threshold is intrinsically difficult to identify in high- β lasers, which makes approaches in terms of photon-statistics spectroscopy very interesting for such systems. In fact, there exist several proposals and techniques aiming at identifying the lasing threshold for such systems, but most of them require complicated experimental setups [28], are only suitable for stabilized continuous-wave operation [29], or can only be applied under nonstationary excitation conditions [30]. Using the excitation photon statistics as an additional degree of freedom may help to characterize the response and lasing transition in such systems in more detail. However, clear-cut criteria to identify the lasing threshold, which is

not necessarily identical to the threshold in the input-output curve, by means of photon-statistics excitation spectroscopy still need to be found. Therefore, it might be worthwhile to investigate the response of nonlinear systems to light fields with different photon statistics, for example, squeezed light, in further studies. Also, characterizing nonlinearities in terms of higher-order correlation functions may provide further insights.

VI. CONCLUSIONS

In conclusion, we studied the influence of the excitation photon number statistics on the mean output photon numbers and the output number photon statistics of linear and nonlinear systems. We have shown that nonlinearities can introduce additional noise which is very sensitive to the input photon number distribution, and that it is possible to identify these nonlinearities by changing the input photon statistics even before the average input photon numbers reach the threshold. Finally, we would like to stress that just as the most suitable description of a light field is given in terms of the response of an arbitrary number of detectors to the light field in terms of correlation functions up to arbitrary order [31], the most suitable description of the response of a system is given in terms of its response (also up to arbitrary order) to a multitude of input states.

ACKNOWLEDGMENTS

This work was supported by the Deutsche Forschungsgemeinschaft through research Grant No. DFG 1549/19-1.

- [1] U. M. Titulaer and R. J. Glauber, *Phys. Rev. B* **140**, 676 (1965).
 [2] P. Michler, A. Imamoğlu, M. D. Mason, P. J. Carson, G. F. Strouse, and S. K. Buratto, *Nature (London)* **406**, 968 (2000).
 [3] S. M. Ulrich, C. Gies, S. Ates, J. Wiersig, S. Reitzenstein, C. Hofmann, A. Löffler, A. Forchel, F. Jahnke, and P. Michler,

Phys. Rev. Lett. **98**, 043906 (2007).

- [4] J. Wiersig, C. Gies, F. Jahnke, M. Abmann, T. Berstermann, M. Bayer, C. Kistner, S. Reitzenstein, C. Schneider, S. Höfling, A. Forchel, C. Kruse, J. Kalden, and D. Hommel, *Nature (London)* **460**, 245 (2009).

- [5] J. Kasprzak, M. Richard, A. Baas, B. Deveaud, R. André, J.-P. Poizat, and L. S. Dang, *Phys. Rev. Lett.* **100**, 067402 (2008).
- [6] M. Aßmann, J.-S. Tempel, F. Veit, M. Bayer, A. Rahimi-Iman, A. Löffler, S. Höfling, S. Reitzenstein, L. Worschech, and A. Forchel, *Proc. Natl. Acad. Sci. USA* **108**, 1804 (2011).
- [7] B. J. Berne and R. Pecora, *Dynamic Light Scattering. With Applications to Chemistry, Biology, and Physics* (Wiley, New York, 1976).
- [8] D. Magde, E. Elson, and W. W. Webb, *Phys. Rev. Lett.* **29**, 705 (1972).
- [9] M. Kira and S. W. Koch, *Phys. Rev. A* **73**, 013813 (2006).
- [10] S. W. Koch, M. Kira, G. Khitrova, and H. M. Gibbs, *Nat. Mater.* **5**, 523 (2006).
- [11] A. Carmele, A. Knorr, and M. Richter, *Phys. Rev. B* **79**, 035316 (2009).
- [12] D. V. Regelman, U. Mizrahi, D. Gershoni, E. Ehrenfreund, W. V. Schoenfeld, and P. M. Petroff, *Phys. Rev. Lett.* **87**, 257401 (2001).
- [13] H. J. Lee, I.-H. Bae, and H. S. Moon, *J. Opt. Soc. Am. A* **28**, 560 (2011).
- [14] J. Kabuss, A. Carmele, M. Richter, W. W. Chow, and A. Knorr, *Phys. Status Solidi B* **248**, 872 (2011).
- [15] A. Carmele, M. Richter, W. W. Chow, and A. Knorr, *Phys. Rev. Lett.* **104**, 156801 (2010).
- [16] T. Altevogt, H. Puff, and R. Zimmermann, *Phys. Rev. A* **56**, 1592 (1997).
- [17] Y. Yamamoto and T. Mukai, *Opt. Quantum Electron.* **21**, 1 (1989).
- [18] M. Aßmann, F. Veit, M. Bayer, M. van der Poel, and J. M. Hvam, *Science* **325**, 297 (2009).
- [19] M. J. Stevens, B. Baek, E. A. Dauler, A. J. Kerman, R. J. Molnar, S. A. Hamilton, K. K. Berggren, R. P. Mirin, and S. W. Nam, *Opt. Express* **18**, 1430 (2010).
- [20] P. R. Rice and H. J. Carmichael, *Phys. Rev. A* **50**, 4318 (1994).
- [21] C. Gies, J. Wiersig, M. Lorke, and F. Jahnke, *Phys. Rev. A* **75**, 013803 (2007).
- [22] S. Strauf, K. Hennessy, M. T. Rakher, Y.-S. Choi, A. Badolato, L. C. Andreani, E. L. Hu, P. M. Petroff, and D. Bouwmeester, *Phys. Rev. Lett.* **96**, 127404 (2006).
- [23] C. Gies, J. Wiersig, and F. Jahnke, *Phys. Rev. Lett.* **101**, 067401 (2008).
- [24] M. Aßmann, F. Veit, M. Bayer, C. Gies, F. Jahnke, S. Reitzenstein, S. Höfling, L. Worschech, and A. Forchel, *Phys. Rev. B* **81**, 165314 (2010).
- [25] S. Reitzenstein, C. Böckler, A. Bazhenov, A. Gorbunov, A. Löffler, M. Kamp, V. D. Kulakovskii, and A. Forchel, *Opt. Express* **16**, 4848 (2008).
- [26] M. Nomura, N. Kumagai, S. Iwamoto, Y. Ota, and Y. Arakawa, *Opt. Express* **17**, 15975 (2009).
- [27] Q. H. Song, L. Ge, A. D. Stone, H. Cao, J. Wiersig, J.-B. Shim, J. Unterhinninghofen, W. Fang, and G. S. Solomon, *Phys. Rev. Lett.* **105**, 103902 (2010).
- [28] M. Aßmann, F. Veit, J.-S. Tempel, T. Berstermann, H. Stolz, M. van der Poel, J. M. Hvam and M. Bayer, *Opt. Express* **18**, 20229 (2010).
- [29] S. Ates, C. Gies, S. M. Ulrich, J. Wiersig, S. Reitzenstein, A. Löffler, A. Forchel, F. Jahnke, and P. Michler, *Phys. Rev. B* **78**, 155319 (2008).
- [30] X. Hachair, R. Braive, G. L. Lippi, D. Elvira, L. Le Gratiet, A. Lemaitre, I. Abram, I. Sagnes, I. Robert-Philip, and A. Beveratos, *Phys. Rev. A* **83**, 053836 (2011).
- [31] R. J. Glauber, *Phys. Rev.* **131**, 2766 (1963).